CrossMark

Bidentate iron complexes based on hyperbranched salicylaldimine ligands and their catalytic behavior toward ethylene oligomerization

Cui-Qin Li[1] · Feng-Feng Wang[1] · Rui Gao[1] · Peng Sun[1] · Na Zhang[1] ·
Jun Wang[1]

Abstract A series of bidentate iron complexes based on hyperbranched salicylaldimine ligands were synthesized and characterized by spectroscopic and analytical methods. Upon activation with methylaluminoxane (MAO), the complexes showed good activities [up to 8.17×10^4 g/(mol Fe h)] for ethylene oligomerization. Activation of the bidentate iron complex with a 1-octadecyl moiety in the ligand backbone (complex **C3**) with Et$_2$AlCl produced higher catalytic activity than **C3** with MAO, although the selectivity for C$_{8+}$ oligomers was lower. The choice of solvent and reaction parameters significantly affected both the activities and selectivities of these complexes. Under the conditions ([Fe] = 5 μmol; temperature = 25 °C; toluene = 50 mL; time = 30 min; ethylene pressure = 0.5 MPa; MAO as cocatalyst), complex **C3** gave high activity [7.46×10^4 g/(mol Fe h)] with better selectivity for C$_{8+}$ oligomers (26.58%). The catalytic activities and selectivities were also influenced by the ligand structure and choice of metal. The catalytic activities declined with increasing alkyl chain length of the ligand backbone. Compared to the nickel complex with 1-tetradecyl as core in the ligand backbone (**C4**), the iron complexes exhibited lower catalytic activities but the better selectivities for C$_{10+}$ oligomers.

✉ Cui-Qin Li
dqpiliciqin@126.com

[1] Provincial Key Laboratory of Oil and Gas Chemical Technology, College of Chemistry and Chemical Engineering, Northeast Petroleum University, Daqing, Heilongjiang, China

Introduction

Ethylene oligomerization is an important catalytic process for the production of linear α-olefins, which are extensively used in the preparation of lubricants, plasticizers, detergents and surfactants, as well as comonomers for the synthesis of linear low-density polyethylene [1]. Initial discovery of the so-called nickel effect by Ziegler leading to ethylene polymerization [2] and oligomerization [3] triggered intensive efforts to develop new homogeneous late transition metal catalysts. Such catalysts can tolerate a range of polar functional groups and even water, which tends to poison traditional Ziegler–Natta/metallocene catalysts. Development of iron and cobalt catalysts in particular was sparked by the independent reports [4–7] of Gibson and Brookhart on bis(arylimino)pyridine iron and cobalt as catalysts for ethylene oligomerization and polymerization, leading to highly linear products. Moreover, the iron and cobalt complexes have high activities and selectivities for α-olefins [5, 6].

Iron-based catalysts are gaining much attention in various organic transformations due to the abundance, low toxicity and low cost of this metal. Following investigations of the iron active species [8], it is generally accepted catalytic iron species should possess a 14e configuration akin to that involved in metallocenes [9] and nickel-based catalysts [10]. For this reason, there have been a number of investigations into iron-based complexes bearing modified bis(imino)pyridine derivatives [11]. Apart from iron(II) complexes of bis(imino)pyridines ligands, other highly active iron complexes have been explored through the development of sp^2-nitrogen tridentate [12, 13] and sp^2-nitrogen bidentate ligands [14]. Following on from these studies, variation of the substituents has allowed access not only to high catalytic activities, but also to the potential

commercialization of systems for ethylene oligomerization and/or polymerization.

These considerations suggest that the structure of the ligand plays a major role in producing effective catalysts. One such ligand type is salicylaldimine, which has been used to prepare effective nickel ethylene polymerization catalysts [15]. The salicylaldimine ligand has the ability to coordinate metals through hard nitrogen and oxygen donor atoms, which leads to better stabilization of metal complexes against reduction and usually good thermal stabilities [16]. Our groups [17] have synthesized dendritic salicylaldimine nickel-based complexes with 1.0 generation dendritic polyamide-amine as a bridging group and investigated their potential for ethylene oligomerization. Upon activation with methylaluminoxane (MAO), the complex exhibited high activity and selectivity for C_{10}–C_{14} products. Following this study, we [18] have also synthesized hyperbranched salicylaldimine nickel catalysts with an octane alkyl group at one end. The catalytic activity reached up to 5.59×10^5 g/(mol Ni h) with MAO as the cocatalyst, and the main products were longer-chain oligomers (C_{10}–C_{18}). However, there are very few salicylaldimine iron catalysts [19, 20]. The few known examples have been used in atom transfer radical polymerization (ATRP) [19]. Our group [20] have synthesized iron complexes with hyperbranched salicylaldimine ligands and investigated the influence of the molecular cavity within the catalyst structure on ethylene oligomerization. These iron coordination complexes, when activated with MAO, exhibited moderate activities in ethylene oligomerization. Therefore, we have synthesized three bidentate iron complexes based on hyperbranched salicylaldimine ligands and investigated their properties as catalysts for ethylene oligomerization. The catalytic reaction parameters, length of alkyl chain of the ligand backbone and the choice of metal center on their catalytic activities have been investigated in detail. Good catalytic activities toward ethylene oligomerization were observed in the presence of MAO.

Experimental

Materials and instrumentation

The reactions of air- and/or moisture-sensitive compounds were performed under a nitrogen atmosphere using standard Schlenk techniques [21]. All solvents were of analytical grade and were dried and distilled prior to use. Methylaluminoxane (10 wt% in toluene) and diethylaluminum chloride (25 wt% in toluene) were purchased from Sigma-Aldrich. Toluene and methanol were provided by the Tianjin Kermel Chemical Reagent Co., Ltd. Salicylaldehyde was obtained from the Tianjin Guangfu Fine

Chemical Research Institute. Generation 1.0 hyperbranched macromolecules with 1-tetradecyl as core (R_{14}-1.0G), with 1-hexadecyl as core (R_{16}-1.0G) and with 1-octadecyl as core (R_{18}-1.0G) were prepared according to the literature procedures [22]. The hyperbranched salicylaldimine ligands with R_{14}-1.0G as the backbone (**L1**), with R_{16}-1.0G as the backbone (**L2**) and with R_{18}-1.0G as the backbone (**L3**) were synthesized according to the literature procedures [23]. The nickel complex with R_{14}-1.0G as the backbone (**C4**) was synthesized through the reaction between **L1** and anhydrous nickel chloride according to the method described in the literature [23]. FTIR spectra were recorded on a Nicolet FTIR 750 infrared spectrometer using KBr pellets. ^{1}H NMR spectra were obtained using a Varian 400 MHz spectrometer with $CDCl_3$ as the solvent and tetramethylsilane (TMS) as the internal standard. UV–Vis spectra were determined using a UV-1700 UV–Vis spectrophotometer. MS data were collected with a Bruker Apex Ultra 70 FTMS using electrospray ionization (ESI) as the ion source. GC analyses were conducted with a Fuli GC 9720 instrument equipped with flame ionization detector (FID) and a 50-m (0.2 mm i.d., 0.5 μm film thickness) HP-PONA column.
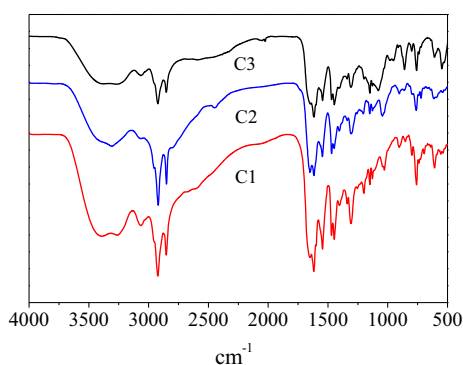
Synthesis of the iron complexes

A solution of iron(II) chloride tetrahydrate (0.11 g, 0.56 mmol) in methanol (5 mL) was added dropwise to a solution of **L1** (0.30 g, 0.46 mmol) in methanol (15 mL) under a nitrogen atmosphere, and the resulting mixture was stirred at 25 °C for 24 h. Diethyl ether (150 mL) was then added, giving a red precipitate. The solid was collected by filtration, washed with cold ether (100 mL) and then dried under vacuum to obtain the iron complex with R_{14}-1.0G as the backbone (**C1**). Yield: 0.31 g (97%). FTIR (KBr cm^{-1}): v (C=N) 1621 (s), v (C–O) 1306 (m), v (N–Fe) 613 (w). Anal. Calcd. for $C_{38}H_{57}N_5FeO_4$: C, 64.85; H, 8.16; N, 9.95. Found: C, 64.79; H, 8.28; N, 9.98%. ESI–MS (*m/z*): 703 [M]$^+$, 649 [M–Fe + H]$^+$, 542 [M–Fe–C_7H_5O + H]$^+$, 452 [M–Fe–$C_{14}H_{29}$ + H]$^+$.

The iron complex with R_{16}-1.0G as the backbone (**C2**) was prepared according to the method described for **C1** using **L2** (0.31 g, 0.46 mmol) and iron(II) chloride tetrahydrate (0.11 g, 0.56 mmol). Yield: 0.32 g (95%). FTIR (KBr cm^{-1}): v (C=N) 1617 (s), v (C–O) 1311 (m), v (N–Fe) 614 (w). Anal. Calcd. for $C_{40}H_{61}N_5FeO_4$: C, 65.65; H, 8.40; N, 9.57. Found: C, 65.29; H, 7.84; N, 9.69%. ESI–MS (*m/z*): 732 [M]$^+$, 678 [M–Fe + H]$^+$, 571 [M–Fe–C_7H_5O + H]$^+$, 465 [M–Fe–$C_{15}H_{31}$ + H]$^+$.
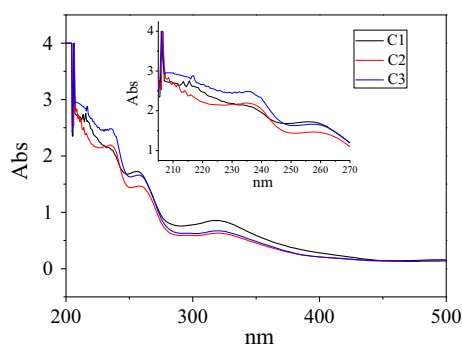
The iron complex with R_{18}-1.0G as the backbone (**C3**) was prepared according to the method described for **C1** using **L3** (0.32 g, 0.46 mmol) and iron(II) chloride tetrahydrate (0.11 g, 0.56 mmol). Yield: 0.33 g (96%).
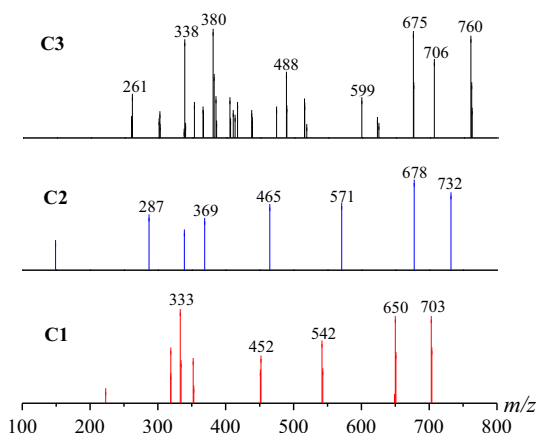
FTIR (KBr cm^{-1}): v (C=N) 1619 (s), v (C–O) 1308 (m), v (N–Fe) 614 (w). Anal. Calcd. for $C_{42}H_{65}N_5FeO_4$: C, 66.39; H, 8.62; N, 9.22. Found: C, 65.80; H, 8.45; N, 9.56%. ESI–MS (m/z): 760 [M]$^+$, 706 [M–Fe + H]$^+$, 599 [M–Fe–C_7H_5O + H]$^+$, 488 [M–Fe–$C_{15}H_{31}$ + H]$^+$.

General procedure for ethylene oligomerization

Ethylene oligomerization was carried out in a 250-mL stainless steel autoclave equipped with a magnetic stirrer and ethylene pressure control system. The reactor was immersed in a bath previously set to the desired temperature and charged with ethylene after removing nitrogen gas under vacuum. A typical reaction was performed by introducing toluene (40 mL) and the required amount of cocatalyst (MAO or Et$_2$AlCl) into the reactor under an ethylene atmosphere. After 20 min, a toluene solution of the catalyst (10 mL, [Fe] = 5 μmol) was injected into the reactor under a stream of ethylene and then the reactor was immediately pressurized. Ethylene was continuously supplied in order to maintain the desired pressure. After 30 min, the reactor was cooled in an ice-water bath and unreacted ethylene was vented. The total volume of the products was determined and the reaction was quenched by addition of 10% HCl in ethanol. The organic phase was collected to investigate the distribution of the products by GC.

Results and discussion

Synthesis of the bidentate iron complexes

We have previously reported the synthesis of a hyperbranched salicylaldimine pro-ligand via a Schiff-base condensation reaction of salicylaldehyde with the first-generation hyperbranched PAMAM [23]. The same synthetic approach was used to prepare the hyperbranched salicylaldimine pro-ligands **L1–L3** (Scheme 1). The progress of the reaction was monitored by FTIR using the v(C=N) band. This band was clearly visible in the FTIR

spectra of all three pro-ligands, in the region of 1619–1621 cm^{-1}. Bands at 3300–3400 cm^{-1} are assigned to the O–H functionalities of the salicylaldimine units. In the ^{1}H NMR spectra of the pro-ligands, the signal for the imine proton was observed around δ 8.33–8.37 ppm. The UV spectra of the hyperbranched salicylaldimine ligands in methanol solution showed three absorption bands at 206, 249 and 315 nm. The band at 206 nm can be assigned to the R band of the C=O $n \rightarrow \pi^*$ transition, while the bands around 249 and 315 nm are most probably due to $\pi \rightarrow \pi^*$ transitions of the benzene rings and $n \rightarrow \pi^*$ transitions of azomethine (C=N), respectively [24]. The mass spectra of **L1**, **L2** and **L3** showed peaks that correspond to [M + H]$^+$ at m/z 650.5, 678.5 and 706.5, respectively. These values are in good agreement with the proposed compositions for these hyperbranched salicylaldimines.

The bidentate iron complexes **C1–C3** were prepared from the pro-ligands **L1–L3** by reaction with iron(II) chloride (Scheme 1). All three complexes were isolated as red solids. They are paramagnetic and could thus not be characterized by NMR spectroscopy. However, other analytical techniques such as FTIR spectra (Fig. 1), UV spectra (Fig. 2) and mass spectra (Fig. 3) confirmed their formulations. Thus, the FTIR spectra of complexes **C1–C3** showed shifts in the v(C=N) and v(C–O) stretching frequencies compared to the free pro-ligands. In the case of the v(C=N) band, the shift was from 1634 (pro-ligand) to 1619 cm^{-1} (complex), while in the case of the v(C–O) band the shift was from 1290 (pro-ligand) to 1308 cm^{-1} (complex). These shifts are consistent with coordination of the ligand to the metal via both the nitrogen and oxygen donor sites. This was further confirmed by v(O–H) bands between 3400 and 3300 cm^{-1}, which are observed in the spectra of the pro-ligands but not those of the complexes. The UV spectra of the iron complexes showed four absorption bands. The three bands observed around 206, 234 and 255 nm are similar to what was observed in the spectra of the pro-ligands, but shifted to lower wavelengths. The weak fourth band at 320 nm can be assigned to forbidden d–d transitions of the metal and resembles what has been seen for other salicylaldimine complexes as

Scheme 1 Synthesis of the hyperbranched salicylaldimine ligands and their bidentate iron complexes

Fig. 1 FTIR spectra of the bidentate iron complexes

Fig. 2 UV spectra of the complexes

Fig. 3 MS spectra of the complexes

reported by Malgas-Enus et al. [15]. The MS of complexes **C1**–**C3** each showed a singly charged molecular ion peak, at *m/z* 703, *m/z* 732 and *m/z* 760, respectively.

To examine the thermal stabilities of the complexes, thermogravimetric analysis was carried out under a nitrogen atmosphere at a heating rate of 10 °C/min from ambient temperature to 1200 °C. The TGA curve for complex **C3** is shown in Fig. 4. The thermal decomposition process of this complex can be subdivided into three stages
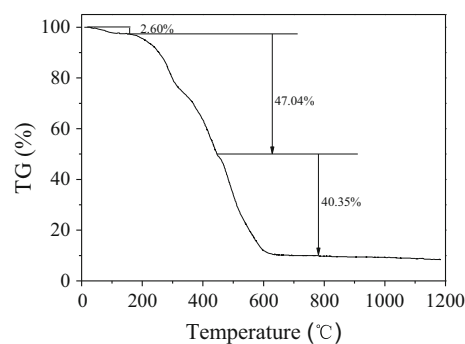
Fig. 4 TGA curve for the complex **C3**

based on the TGA curve. The first stage shows a mass loss of 2.6%, up to 160 °C, and is attributed to the loss of absorbed moisture. The next mass loss in the temperature range of 160–445 °C corresponds to decomposition of the ligand and loss of $-C_{24}H_{45}O_2N$; the observed mass loss of 47.0% is in fair agreement with the calculated value of 50.0%. The final mass loss in the range of 445–780 °C corresponds to complete decomposition of the ligand and loss of ethylenediamine and benzene; the experimental result (40.4%) is in good agreement with the calculated value (40.6%). The residual mass remains almost constant until 800 °C; the residual mass (9.5%) is consistent with assignment of this residue to iron oxide (calc. 10.0%).

Ethylene oligomerization studies

The oligomerization of ethylene catalyzed by these bidentate iron complexes with various cocatalysts and in various solvents has been systematically investigated. Reaction factors such as the molar ratio of cocatalyst to iron complex, the reaction temperature and pressure each have an influence on the activity toward ethylene oligomerization. Before carrying out parallel trials, we assayed the standard deviations for catalytic activity and oligomer distributions under the same conditions (Table 1).

In the past few years, numerous studies have revealed the influence of cocatalyst on catalytic activity, stability,

Table 1 Error analysis for oligomerization reactions with catalyst **C1**

C1	Run 1	Run 2	Run 3	Average	SD
Activity[a]	8.17	8.13	8.20	8.17	0.03
C$_4$	54.45	55.04	55.13	54.87	0.30
C$_6$	19.00	18.95	18.94	18.96	0.03
C$_8$	19.48	19.40	19.38	19.42	0.04
C$_{8+}$	7.07	6.61	6.55	6.74	0.23

Reaction condition: [Fe] = 5 µmol; toluene = 50 mL; time = 30 min; Al/Fe = 500; *T* = 25 °C; ethylene pressure = 0.5 MPa

[a] 10^4 g/(mol Fe h)

polymerization kinetic profile, polymer molecular weight and stereoregularity in cationic transition metal-catalyzed olefin polymerization processes [25]. In order to shed light on the influence of cocatalysts on the catalytic behavior of these bidentate iron complexes, we activated complex C3 using MAO and Et$_2$AlCl in toluene solvent. Since the function of the cocatalyst is to promote formation of the active species in the presence of impurities such as moisture and oxygen, an appropriate amount of cocatalyst is required. It was clear that the choice of aluminum cocatalyst had a significant effect on both the catalytic activity and product distribution (Table 2, entries 2, 13). When activated with MAO, the complex showed moderate activity of up to 7.46×10^4 g/(mol Fe h) and afforded more C$_{8+}$ oligomers (26.58%). The use of Et$_2$AlCl induced higher catalytic activity, but with less selectivity for C$_{8+}$ oligomers (19.23%). Thus, further studies of these complexes for ethylene oligomerization were carried out with MAO as cocatalyst.

The choice of solvent can affect the catalytic activity and product distribution, affecting both the monomer concentration and the solubility of the catalyst itself [26]. With this in mind, the catalytic behavior of complex C3 was investigated in both cyclohexane and n-hexane and compared with the corresponding results in toluene (Table 2, entries 2, 11–12). Under similar conditions, the catalytic activities decreased in the order n-hexane < cyclohexane < toluene. These observations are attributed to the poor solubility of C3 in n-hexane and cyclohexane. It is interesting to note that butenes (62.64%) were predominant products for the system in toluene solvent. However, longer-chain oligomers (53.01%) and hexenes (73.74%) were the major products in cyclohexane and n-hexane solvents, respectively. This trend is consistent with solvent-induced variations in catalytic activities, since higher catalytic activities are more likely to promote chain termination over chain propagation [27].

The preliminary study was extended to investigate the effects of temperature, Al/Fe molar ratio and reaction pressure. The reaction temperature can affect the activity, since ethylene oligomerization is a highly exothermic reaction, and furthermore, the solubility of ethylene and stability of catalytic species are also affected by temperature. The pre-catalyst C3 showed slightly lower oligomerization activity at lower temperature (Table 2, entry 1) compared to the result obtained at 25 °C (Table 2, entry 2). This result can be associated with reduced solubility of C3 in toluene at 15 °C generating lower amounts of active species. Increasing the reaction temperature from 25 to 45 °C led to a loss in the catalytic activity (Table 2, entries 2–4), which might be due to decomposition of the active species and/or lower ethylene solubility at higher temperature. The contents of the oligomeric proportions were randomly changed, implying that the reaction temperature did not rationally control the rate of chain propagation to β-hydrogen elimination.

Table 2 Ethylene oligomerization with catalyst system **C3**

Entry[a]	Al/Fe	T (°C)	P (MPa)	Activity[b]	Oligomer distribution (%)[c]			
					C$_4$	C$_6$	C$_8$	C$_{10}$–C$_{18}$
1	500	15	0.5	6.27	68.75	8.51	17.00	5.74
2	500	25	0.5	7.46	62.64	10.76	15.35	11.23
3	500	35	0.5	5.66	71.99	3.77	10.08	14.16
4	500	45	0.5	4.96	80.11	1.59	9.66	8.64
5	200	25	0.5	4.08	74.47	4.90	11.98	8.65
6	700	25	0.5	5.75	82.06	6.10	9.04	2.80
7	1000	25	0.5	5.13	77.44	8.47	10.59	3.50
8	500	25	0.1	6.76	66.55	14.51	13.67	5.27
9	500	25	0.3	7.25	68.83	7.34	6.20	17.63
10	500	25	0.7	8.63	70.04	8.38	14.29	7.29
11[d]	500	25	0.5	6.23	31.63	7.86	7.50	53.01
12[e]	500	25	0.5	5.13	15.97	73.74	0.69	9.60
13[f]	500	25	0.5	11.02	75.16	5.61	9.36	9.87

[a] Reaction condition: [Fe] = 5 μmol; toluene = 50 mL; time = 30 min; MAO as cocatalyst

[b] 10^4 g/(mol Fe h)

[c] Determined by GC

[d] Cyclohexane as solvent (50 mL)

[e] n-Hexane as solvent (50 mL)

[f] Et$_2$AlCl as cocatalyst (500 equiv)

The effects of the Al/Fe molar ratio on the system were also investigated using **C3**. Increasing the Al/Fe molar ratio in the range 200–1000 resulted in an initial increase and then a gradual decrease (Table 2, entries 2, 5–7), with the highest activity of 7.46×10^4 g/(mol Fe h) observed at an Al/Fe molar ratio of 500 at 25 °C. Higher Al/Fe molar ratios resulted in decreased catalytic activity, possibly due to high accumulation of alkylaluminum impurities which might cause catalyst deactivation [28]. Generally higher Al/Fe molar ratios favored the formation of lower C_4 oligomers. For example, C_4 proportions of 62.64 and 77.44% were observed at Al/Fe molar ratios of 500 and 1000, respectively (Table 2, entries 2, 7). This trend could be attributed to increased chain transfer to the cocatalyst or greater chain termination due to increased catalytic activity [25].

The influence of ethylene concentration was studied by varying ethylene pressure from 0.1 to 0.7 MPa using catalyst **C3** (Table 2, entries 2, 8–10). As expected, increasing the ethylene pressure from 0.1 to 0.7 MPa led to increased catalytic activity from 6.76×10^4 to 8.63×10^4 g/(mol Fe h), respectively. The ethylene concentration also had a significant effect on the product distribution. Increase in ethylene pressure favored the formation of shorter-chain oligomers (C_4 and C_6). Higher proportions of lower fraction oligomers at higher pressures are consistent with increased catalytic activity leading to rapid chain termination [29].

### Influence of catalyst structure on ethylene oligomerization

The influence of complex structure on both the catalytic activity and product distribution was also studied. Under the optimized conditions for the catalytic system employing **C3**, the bidentate nickel complex **C4** (Fig. 5) and all three bidentate iron complexes **C1**–**C3** were investigated for ethylene oligomerization. Most notable was the role of the metal atom in regulating catalytic performance. Compared with the nickel analogue **C4**, the iron complex **C1** displayed lower catalytic activity and higher selectivity for

longer-chain oligomers (Table 3, entries 1, 4). Similar results have been previously reported for nickel and iron complexes of 2-(2-pyridyl) quinoxaline in ethylene oligomerization reactions [30] and can be attributed to electronic factors [31].

We also noted that varying the alkyl substituent on the ligand backbone from a tetradecyl to an octadecyl group led to noticeable decreases in activities in all the catalytic systems (Table 3, entries 1–3). For example, replacing the tetradecyl group (**C1**) with a hexadecyl group (**C2**) resulted in decreased activity from 8.17×10^4 to 7.98×10^4 g/(mol Fe h), respectively, when using MAO as a cocatalyst (Table 3, entries 1, 2). This may be due to bulkier ligands hindering coordination of ethylene to the active metal center. However, random data were observed for the distribution of oligomers produced by the different iron pre-catalysts, suggesting that the degree of steric hindrance on the iron pre-catalysts has little influence on product distribution.

Mechanism of the catalytic oligomerization

Since late transition metal complexes exhibit very high activities for ethylene polymerization and oligomerization, researchers are keen to elucidate the catalytic mechanism. However, due to limitations resulting from the paramagnetism of such iron complexes, their active species are not as well understood as are those of the α-diimine palladium catalysts. Considering the results of this study and previous reports, it is possible to deduce the mechanism of oligomerization at the iron metal center (Fig. 6). On reaction with a cocatalyst (MAO or Et$_2$AlCl), the salicylaldimine iron complex is transformed into an active species, often involving interactions between the metal and a hydride (or alkyl) and ethylene molecule [32]. The iron hydride species can be generated by a variety of standard organometallic reactions including chain propagation and
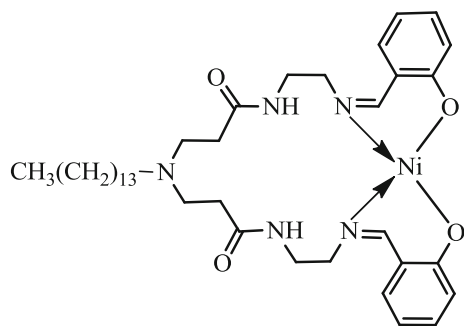
**Fig. 5** Structure of the bidentate nickel complex **C4**

Table 3 Ethylene oligomerization studies with **C1**–**C4** in using MAO as cocatalyst

Entry[a]	Complexes	Activity[b]	Oligomer distribution (%)[c]			
			C_4	C_6	C_8	C_{10}–C_{18}
1	**C1**	8.17	54.45	19.00	19.48	7.07
2	**C2**	7.98	35.54	25.26	25.82	13.08
3	**C3**	7.46	62.64	10.76	15.35	11.23
4	**C4**	13.50	52.10	9.30	32.63	5.97

[a] Reaction condition: [M] = 5 μmol; toluene = 50 mL; time = 30 min; Al/M = 500; T = 25 °C; ethylene pressure = 0.5 MPa

[b] 10^4 g/(mol M h)

[c] Determined by GC
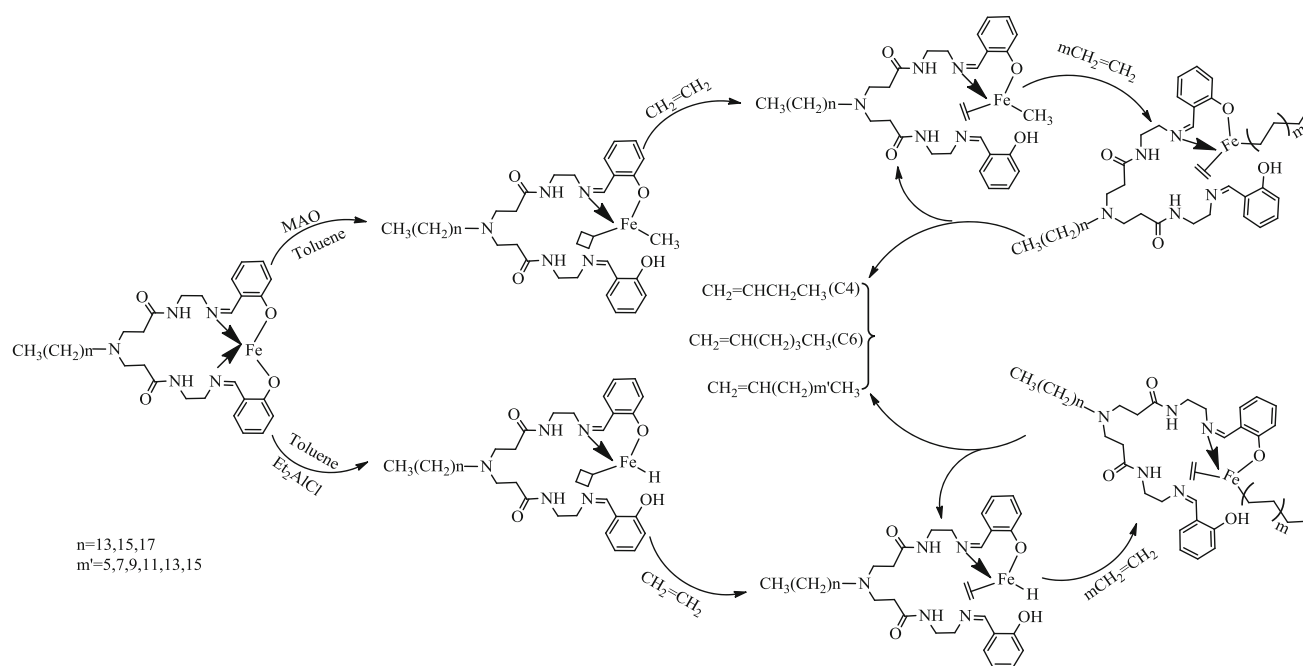
Fig. 6 Proposed mechanism of catalysis by the bidentate iron complexes in ethylene oligomerization

β-hydrogen elimination from an intermediate iron alkyl and oxidative addition of a Lewis acid to a zero-valent iron species [33, 34]. The type of cocatalyst can affect product distribution. With MAO as cocatalyst, the better selectivity for longer-chain oligomers might be due to the fact that the chain propagation is faster than β-hydrogen elimination.

Conclusions

A series of bidentate iron complexes based on hyper-branched salicylaldimine ligands were synthesized and characterized. In the presence of either MAO or Et_2AlCl, the bidentate iron complex **C3** had high catalytic activities for ethylene oligomerization. MAO was found to be a more effective cocatalyst than Et_2AlCl. Among various solvents, toluene was found to be most effective for these bidentate iron complexes. The catalytic activity for ethylene oligomerization and selectivity for oligomers could be easily controlled by altering the reaction conditions such as the temperature, Al/Fe molar ratio and reaction pressure. The catalytic activity and selectivity were also significantly influenced by the ligand structure and choice of metal. The catalytic activities of these bidentate iron complexes decreased with increasing alkyl chain length, and the alkyl chain also had a great influence on the selectivity for ethylene oligomerization. Compared with the nickel ana-logue **C4**, the iron complex **C1** displayed lower catalytic activity and higher selectivity for longer-chain oligomers. While the catalytic activities of these systems are moderate, their superiority lies in their higher selectivities for longer-chain oligomers. In future work, we hope to obtain new oligomerization iron complexes based on hyperbranched salicylaldimine ligands modulating structural and electronic characteristics by the nature of the substituents on the salicylaldehyde moieties in order to improve the catalytic activities.

References

1. Skupinska J (1991) Chem Rev 91:613–648
2. Ziegler K, Gellert HG (1950) Liebigs Ann Chem 567:195–203
3. Ziegler K, Holzkamp E, Martin H, Breil H (1955) Angew Chem 67:541–547
4. Small BL, Brookhart M, Bennett AMA (1998) J Am Chem Soc 120:4049–4050
5. Small BL, Brookhart M (1998) J Am Chem Soc 120:7143–7144
6. Britovsek GJP, Gibson VC, Kimberley BS, Maddox PJ, McTavish SJ, Solan GA, White AJP, Williams DJ (1998) Chem Commun 7:849–850
7. Gibson VC, Redshaw C, Solan GA (2007) Chem Rev 107:1745–1776
8. Fernández I, Trovitch RJ, Lobkovsky E, Chirik PJ (2008) Organometallics 27:109–118
9. Alt HG, Licht EH, Licht AI, Schneider KJ (2006) Coord Chem Rev 250:2–17
10. Simon LC, Mauler RS, De Souza RF (1999) J Polym Sci A: Polym Chem 37:4633–4656

11. Bianchini C, Giambastiani G, Luconi L, Meli A (2010) Coord Chem Rev 254:431–455
12. Xiao LW, Gao R, Zhang M, Li Y, Cao XP, Sun WH (2009) Organometallics 28:2225–2233
13. Sun WH, Hao P, Li G, Zhang S, Wang WQ, Yi JJ, Asma M, Tang N (2007) J Organomet Chem 692:4506–4518
14. Xiao TPF, Zhang S, Kehr G, Hao X, Erker G, Sun WH (2011) Organometallics 30:3658–3665
15. Malgas-Enus R, Mapolie SF (2014) Inorg Chim Acta 409:96–105
16. Eaves R, Parkin S, Ladipo FT (2007) Inorg Chem 46:9495–9502
17. Wang J, Zhang P, Chen S, Li CQ, Li HY, Yang G (2013) J Macro Sci Part A 50:163–167
18. Wang J, Yang G, Li CQ, Shi WG (2014) Chem J Chin Univ 35:1536–1540
19. O'Reilly RK, Gibson VC, White AJP, Williams DJ (2003) J Am Chem Soc 125:8450–8451
20. Zhang N, Wang SH, Song L, Li CQ, Wang J (2016) Inorg Chim Acta 453:369–375
21. Shriver DF (1986) The manipulation of air-sensitive compounds. McGraw-Hill, New York
22. Wang J, Li CQ, Zhang SY, Sun F, Ge TJ (2008) Chin Chem Lett 19:43–46
23. Li CQ, Yu HY, Lin ZY, Wang FF, Zhang N, Wang J (2017) J Coord Chem. doi:10.1080/00958972.2017.1293822
24. Tas E, Kilic A, Konak N, Yilmaz I (2008) Polyhedron 27:1024–1032
25. Chen EY, Marks TJ (2000) Chem Rev 100:1391–1434
26. Chandran D, Kwak CH, Oh JM, Ahn IY, Ha CS, Kim I (2008) Catal Lett 125:27–34
27. Doherty MD, Trudeau S, White PS, Morken JP, Brookhart M (2007) Organometallics 26:1261–1269
28. Abbo HS, Titinchi SJ (2013) Molecules 18:4728–4738
29. Killian CM, Johnson LK, Brookhart M (1997) Organometallics 16:2005–2007
30. Shao CX, Sun WH, Li ZL, Hu YL, Han LQ (2002) Catal Commun 3:405–410
31. Laine TV, Lappalainen K, Liimatta J, Aitola E, Löfgren B, Leskelä M (1999) Macromol Rapid Commun 20:487–491
32. Jolly PW (1982) In: Wilkinson G, Stone FGA, Abel EW (eds) Comprehensive organometallic chemistry, vol 8. Pergamon Press, Oxford, p 615
33. Carlini C, Isola M, Liuzzo V, Galletti AMR, Sbrana G (2002) Appl Catal A: Gen 231:307–320
34. Kim I, Kwak CH, Kim JS, Ha CS (2005) Appl Catal A: Gen 287:98–107